

Curvature Effects in Thin Magnetic Shells

Yuri Gaididei,^{1,*} Volodymyr P. Kravchuk,^{1,†} and Denis D. Sheka^{2,‡}

¹*Bogolyubov Institute for Theoretical Physics, Kiev 03143, Ukraine*

²*Taras Shevchenko National University of Kiev, Kiev 01601, Ukraine*

(Received 10 December 2013; revised manuscript received 23 April 2014; published 25 June 2014)

A magnetic energy functional is derived for an arbitrary curved thin shell on the assumption that the magnetostatic effects can be reduced to an effective easy-surface anisotropy; it can be used for solving both static and dynamic problems. General static solutions are obtained in the limit of a strong anisotropy of both signs (easy-surface and easy-normal cases). It is shown that the effect of the curvature can be treated as the appearance of an effective magnetic field, which is aligned along the surface normal for the case of easy-surface anisotropy and is tangential to the surface for the case of easy-normal anisotropy. In general, the existence of such a field excludes the solutions that are strictly tangential or strictly normal to the surface. As an example, we consider static equilibrium solutions for a cone surface magnetization.

DOI: 10.1103/PhysRevLett.112.257203

PACS numbers: 75.70.-i, 75.10.Hk, 75.30.Et

Recent advances in microstructuring technology have made it possible to fabricate various low-dimensional systems with complicated geometry. Examples are cylindrical high-mobility two-dimensional (2D) electron structures obtained by rolling up mismatched semiconductor layers [1], flexible electronic devices [2] and integrated circuits [3], spin-wave interference in rolled-up ferromagnetic microtubes [4], magnetically capped rolled-up nanomembranes [5], etc. After the seminal work of da Costa [6]—where an effective Schrödinger equation for the tangential motion of a particle rigidly bounded to a surface was derived and the presence of effective surface potentials depending on both the Gaussian and mean curvatures was shown—much work has been done to elucidate the curvature effects on charge and energy transport and localization in systems with complicated geometry [7]. The behavior of vector and tensor fields on curved surfaces has attracted the attention of many researchers (see, e.g., Refs. [8,9]). However, despite the amount of work that has been done it is not fully understood. One of the reasons for this is a complicated and intimate relationship between two geometries: the geometry of the field (the director in liquid crystalline phases, the magnetization vector in ferromagnets, the displacement vector in crystalline monolayers, etc.) and the geometry of the underlying substrate. Until now researchers in this area were mostly concerned with the case when the vector field is strictly tangential to the curved surface, i.e., 2D vector fields. This approach showed its validity and robustness in understanding crystalline arrangements of particles interacting on a curved surface [8,10,11], in studying the geometric interaction between defects and curvature in thin layers of superfluids, superconductors, and liquid crystals deposited on curved surfaces [12], and in the frustrated nematic order in spherical geometries [13]. However, the tangentiality condition may be too restrictive for magnetic systems with their different

types and strengths of surface anisotropy (in/out of surface). Moreover, in the frame 2D vector-field approach it is impossible to study the dynamical properties of magnets on curved surfaces.

The goal of this Letter is to develop a full three-dimensional (3D) approach for thin magnetic shells of arbitrary shape.

The phenomenological study of nanomagnets is based on the classical Landau-Lifshitz equation $\dot{\mathbf{m}} = [\mathbf{m} \times \delta E / \delta \mathbf{m}]$, where $\mathbf{m} = \mathbf{M} / M_s$ is the normalized magnetization unit vector with M_s being the saturation magnetization, E is the rescaled energy, normalized by $4\pi M_s^2$, and the overdot indicates a derivative with respect to the rescaled time in units of $(4\pi\gamma M_s)^{-1}$, where γ is the gyromagnetic ratio. No damping is taken into account. Since the dynamics of the vector \mathbf{m} is a precessional one, the energy functional \mathcal{E} must be written for the case of a general—not necessarily tangential—magnetization distribution. Note that in the case of a static tangential distribution of the director in a curvilinear nematic shell the general expression for the surface energy was recently obtained in Refs. [14,15]. The expressions for E for an arbitrary three-dimensional magnetization distribution have already been obtained only for cylindrical [16,17] and spherical [18] geometries. Here we propose a general approach that can be used for an arbitrary curvilinear surface and an arbitrary magnetization vector field. However, we neglect dipole-dipole interactions and take into account only exchange and anisotropy contributions. The last one can have a symmetry of the surface; e.g., it can be uniaxial with the axis oriented along the surface normal.

First of all, we define a set of geometrical parameters of a curvilinear surface which will affect the physical properties of the magnetic system. Considering a 2D surface \mathcal{S} embedded in 3D space \mathbb{R}^3 , we use its parametric representation of the general form $\mathbf{r} = \mathbf{r}(\xi_1, \xi_2)$, where $\mathbf{r} = x_i \hat{\mathbf{x}}_i$

is the 3D position vector defined in the Cartesian basis $\hat{\mathbf{x}}_i \in \{\hat{\mathbf{x}}, \hat{\mathbf{y}}, \hat{\mathbf{z}}\}$, and ξ_α are local curvilinear coordinates on the surface. Here and below, latin indices $i, j = 1, 2, 3$ describe Cartesian coordinates and Cartesian components of vector fields, whereas greek indices $\alpha, \beta = 1, 2$ numerate curvilinear coordinates and curvilinear components of vector fields. We also use here the Einstein summation convention.

Let us introduce the local normalized curvilinear basis $\mathbf{e}_\alpha = \mathbf{g}_\alpha / |\mathbf{g}_\alpha|$, $\mathbf{n} = [\mathbf{e}_1 \times \mathbf{e}_2]$, where $\mathbf{g}_\alpha = \partial_\alpha \mathbf{r}$ with $\partial_\alpha = \partial / \partial \xi_\alpha$. The following analysis is performed under the assumption that the basis is orthogonal or, equivalently, that the metric tensor $g_{\alpha\beta} = \mathbf{g}_\alpha \cdot \mathbf{g}_\beta$ is diagonal. For convenience we introduce the vector $\boldsymbol{\omega}$ of the spin connection $\boldsymbol{\omega}_\alpha = \mathbf{e}_1 \cdot \partial_\alpha \mathbf{e}_2$, the second fundamental form $b_{\alpha\beta} = \mathbf{n} \cdot \partial_\beta \mathbf{g}_\alpha$, and the matrix $\|h_{\alpha\beta}\| = \|b_{\alpha\beta} / \sqrt{g_{\alpha\alpha}g_{\beta\beta}}\|$ which has the properties of the Hessian matrix: the Gauss curvature $\mathcal{K} = \det(h_{\alpha\beta})$ and the mean curvature $\mathcal{H} = \text{tr}(h_{\alpha\beta})/2$.

Physically realizable magnetic nanomembranes are of a finite thickness L . We model such a nanomembrane as a thin shell with $L \ll \mathcal{R}$, with \mathcal{R} being the minimal curvature radius of the surface \mathcal{S} . Then the space domain filled by the shell can be parametrized as $\mathbf{r}(\xi_1, \xi_2, \eta) = \mathbf{r}(\xi_1, \xi_2) + \eta \mathbf{n}(\xi_1, \xi_2)$, where $\eta \in [-L/2, L/2]$. The main assumption is that the thickness L is small enough to ensure that the magnetization is uniform along the direction of the normal; i.e., we assume that $\mathbf{m} = \mathbf{m}(\xi_1, \xi_2)$. This assumption is appropriate for the cases when the thickness is much smaller than the characteristic magnetic length. Similarly to Refs. [14,15], we derive the effective 2D magnetic energy of the shell as a limiting case $L \rightarrow 0$ of the 3D model and only consider contributions to the magnetic energy that are linear with respect to the thickness L . Thus we consider the surface magnetic energy in the form

$$E = L \int_{\mathcal{S}} [\ell^2 \mathcal{E}_{\text{ex}} + \lambda (\mathbf{m} \cdot \mathbf{n})^2] d\mathcal{S}, \quad (1)$$

where the integration is over the surface \mathcal{S} with the surface element $d\mathcal{S} = \sqrt{g} d\xi_1 d\xi_2$, where $g = \det(g_{\alpha\beta})$. The second term in the integrand is the density of the anisotropy energy; it is of easy-surface or easy-normal type for the cases $\lambda > 0$ and $\lambda < 0$, respectively, where λ is the normalized anisotropy coefficient. For examples of curved magnets with both kinds of anisotropies see Refs. [19–21]. The only curvature effect on the anisotropy term is a spatial dependence of the anisotropy axis oriented along the normal vector \mathbf{n} . The exchange energy density is represented by the first term, where $\ell = \sqrt{A/(4\pi M_s^2)}$ is the exchange length and A is the exchange constant. The length scale in the system (1) is determined by the parameter $\sigma = \ell / \sqrt{|\lambda|}$, which is a domain-wall width.

It has been well established in numerous studies on rigorous micromagnetism (see, e.g., Refs. [22–24]) that the effects of nonlocal dipole-dipole interactions can be

reduced to an effective easy-surface anisotropy for thin shells when the thickness is much less than the exchange length and size of the system. Being aware that these results were obtained for plane films, we assume that the same arguments are valid for smoothly curved shells [25].

In the Cartesian frame of reference the exchange energy density $\mathcal{E}_{\text{ex}} = (\nabla m_i)(\nabla m_i)$. The Cartesian components of the magnetization vector m_i are expressed in terms of the curvilinear components m_α and m_n as follows: $m_i = m_\alpha (\mathbf{e}_\alpha \cdot \hat{\mathbf{x}}_i) + m_n (\mathbf{n} \cdot \hat{\mathbf{x}}_i)$. Then we substitute this expression into \mathcal{E}_{ex} and apply the gradient operator in its curvilinear form, $\nabla \equiv (g_{\alpha\alpha})^{-1/2} \mathbf{e}_\alpha \partial_\alpha$. To incorporate the constraint $|\mathbf{m}| = 1$, we also use the angular parametrization

$$\mathbf{m} = \sin \theta \cos \phi \mathbf{e}_1 + \sin \theta \sin \phi \mathbf{e}_2 + \cos \theta \mathbf{n}, \quad (2)$$

where $\theta = \theta(\xi_1, \xi_2)$ is the colatitude and $\phi = \phi(\xi_1, \xi_2)$ is the azimuthal angle in the local frame of reference. Finally, in terms of θ and ϕ the exchange energy density \mathcal{E}_{ex} reads

$$\mathcal{E}_{\text{ex}} = [\nabla \theta - \boldsymbol{\Gamma}(\phi)]^2 + \left[\sin \theta (\nabla \phi - \boldsymbol{\Omega}) - \cos \theta \frac{\partial \boldsymbol{\Gamma}(\phi)}{\partial \phi} \right]^2. \quad (3)$$

Here the vector $\boldsymbol{\Omega} = (\boldsymbol{\omega}_1 / \sqrt{g_{11}}, \boldsymbol{\omega}_2 / \sqrt{g_{22}})$ is a modified spin connection and the vector $\boldsymbol{\Gamma}$ is determined as follows:

$$\boldsymbol{\Gamma}(\phi) = \|h_{\alpha\beta}\| \boldsymbol{\tau}(\phi) = \mathcal{H} \boldsymbol{\tau}(\phi) + \sqrt{\mathcal{H}^2 - \mathcal{K}} \boldsymbol{\tau}(\nu - \phi), \quad (4)$$

where $\boldsymbol{\tau}(\phi) = (\cos \phi, \sin \phi)$ and $\tan \nu = 2h_{12}/(h_{11} - h_{22})$. Note that $\boldsymbol{\Gamma}$ vanishes in the case of a planar film and the expression (3) is reduced to the well-known formula $\mathcal{E}_{\text{ex}} = (\nabla \theta)^2 + \sin^2 \theta (\nabla \phi - \boldsymbol{\Omega})^2$ [26]. It should be emphasized that the general expression (3) is reduced to the already obtained results for the specific cases of cylindrical [16,17] and spherical [18] geometries.

Using the energy expression (3), one can analyze general static solutions for the case of a strong anisotropy. Let us first consider the case of an easy-surface anisotropy ($\lambda > 0$) and let the anisotropy be strong enough to provide a quasitangential magnetization distribution; in other words, $\theta = \pi/2 + \vartheta$ with $\vartheta \ll 1$. Then the total energy (1) can be expressed as

$$E \approx L \int (\ell^2 \mathcal{E}^t + 2\ell^2 F^t \vartheta + \lambda \vartheta^2) d\mathcal{S},$$

$$\mathcal{E}^t = \boldsymbol{\Gamma}^2 + (\nabla \phi - \boldsymbol{\Omega})^2, F^t = \nabla \cdot \boldsymbol{\Gamma} + (\nabla \phi - \boldsymbol{\Omega}) \frac{\partial \boldsymbol{\Gamma}}{\partial \phi}, \quad (5)$$

where \mathcal{E}^t is the energy density of a strictly tangential distribution ($\theta \equiv \pi/2$, or equivalently $m_n \equiv 0$) and F^t can be treated as the amplitude of a curvature-induced effective magnetic field oriented along the normal vector \mathbf{n} . Note that $F^t \equiv 0$ in the case of planar film.

The minimization of the energy functional (5) results in

$$\vartheta = -\sigma^2 F^t(\phi) + \mathcal{O}(\sigma^4), \quad (6)$$

where the equilibrium function ϕ is obtained as a solution of the equation $\delta\mathcal{E}^t/\delta\phi = 0$. According to Eq. (6), the strictly tangential solution is realized only for a specific case, $F^t(\phi) \equiv 0$.

An expression analogous to \mathcal{E}^t was recently obtained in Refs. [14,15] for the case of curvilinear nematic shells with a purely tangential distribution of the director. However, as follows from Eq. (6), the purely tangential solutions are not possible in the general case.

For the opposite case of a strong easy-normal anisotropy ($\lambda < 0$) one has two possibilities, namely, $\theta = \vartheta$ or $\theta = \pi - \vartheta$ with $\vartheta \ll 1$. In the first case the total energy (1) can be written as

$$E \approx L \int (2\ell^2 \vartheta F^n + |\lambda|\vartheta^2) d\mathcal{S} + \text{const}, \quad (7)$$

where $F^n = (\nabla \cdot h) \cdot \boldsymbol{\tau} + \boldsymbol{\Omega}(h(\partial\boldsymbol{\tau}/\partial\phi))$ can be treated as the amplitude of a curvature-induced effective magnetic field oriented along the vector $\boldsymbol{\tau}$, where $(\nabla \cdot h)_\alpha = (1/\sqrt{g})\partial_\beta(h_{\beta\alpha}\sqrt{g/g_{\beta\beta}})$ is a tensor generalization of the divergence. Note that $F^n \equiv 0$ in the case of a planar film.

The minimization of the energy functional (7) leads to the solution

$$\vartheta = -\sigma^2 F^n(\phi) + \mathcal{O}(\sigma^4), \quad \tan \phi = \frac{(\nabla \cdot h)_2 - (h\boldsymbol{\Omega})_1}{(\nabla \cdot h)_1 + (h\boldsymbol{\Omega})_2}. \quad (8)$$

There are two equilibrium values of the azimuthal angle: ϕ and $\phi + \pi$. One should choose the solution that provides $\vartheta > 0$.

Similarly to the previous case, a solution strictly normal to the surface is realized only for the specific case $F^n \equiv 0$. This is the case for spherical and cylindrical surfaces.

As an example of an application of our theory we find the possible equilibrium states of cone shells with high anisotropies of different types. We consider here the side surface of a right circular truncated cone. The radius of the truncation face is R and the length of the cone's generatrix is w . By varying the generatrix inclination angle $0 \leq \psi \leq \pi/2$ one can continuously proceed from the planar ring ($\psi = 0$) to the cylinder surface ($\psi = \pi/2$); see Fig. 1. We chose the following parametrization of the cone surface:

$$x + iy = (R + r \cos \psi) \exp(i\chi), \quad z = r \sin \psi, \quad (9)$$

where the curvilinear coordinates $\chi \in [0, 2\pi)$ and $r \in [0, w]$ play the roles of ξ_1 and ξ_2 , respectively. The definition (9) generates the following geometrical properties of the surface: the metric tensor $\|g_{\alpha\beta}\| = \text{diag}(g, 1)$, the modified

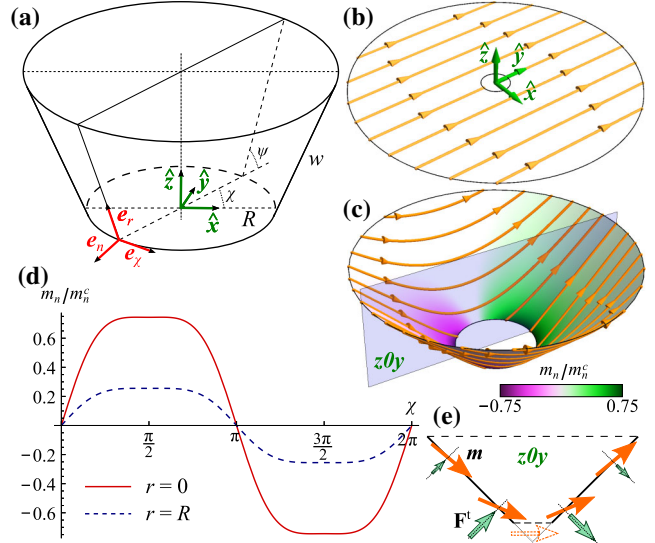


FIG. 1 (Color online) (color online). Onion state of a cone surface. a) Geometry and notations. Panels b) and c) show the onion solution (11) for $\psi = 0$ and $\psi = \pi/4$, respectively, including the in-surface magnetization distribution (by streamlines) and the normal component m_n , normalized by $m_n^c = \sigma^2/R^2$ (by color scheme). d) Variation of m_n along the azimuthal direction \mathbf{e}_χ for a cone with $\psi = \pi/4$. e) Schematic distributions of the magnetization \mathbf{m} and effective curvature field \mathbf{F}^t within the cut plane $z=0y$.

spin connection $\boldsymbol{\Omega} = \mathbf{e}_\chi \cos \psi / \sqrt{g}$, and the second fundamental form $\|b_{\alpha\beta}\| = \text{diag}(-\sin \psi \sqrt{g}, 0)$, where $\sqrt{g} = R + r \cos \psi$. In accordance with Eq. (4) $\boldsymbol{\Gamma} = -\mathbf{e}_\chi \sin \psi \cos \phi / \sqrt{g}$.

In the case of a strong easy-surface anisotropy, the energy of the pure tangential distribution is

$$\mathcal{E}^t = \frac{1}{g} [\sin^2 \psi \cos^2 \phi + (\partial_\chi \phi - \cos \psi)^2] + (\partial_r \phi)^2. \quad (10)$$

The minimization of the energy results in $\phi = \phi(\chi)$, which satisfies the pendulum equation for $\phi'' + \frac{1}{2} \sin^2 \psi \sin 2\phi = 0$. The obtained magnetization state is analogous to the well-known onion state with transverse domain walls [27], so we use this name for the solution,

$$\phi^{\text{on}}(\chi) = \text{am}(x, k), \quad x = \frac{2\chi}{\pi} K(k), \quad (11)$$

where $\text{am}(x, k)$ is the Jacobi amplitude [28] and the modulus k is determined by $2kK(k) = \pi \sin \psi$, with $K(k)$ being the complete elliptic integral of the first kind [28]. It should be noted that in the planar limit $\psi \rightarrow 0$ the onion solution (11) is reduced to $\phi^{\text{on}} = \chi$, which corresponds to a uniform magnetization distribution [29] in the Cartesian frame of reference; see Fig. 1(b). The solution of Eq. (11) that corresponds to $\psi = \pi/4$ is shown in Fig. 1(c). Finally, the energy (1) of the onion state (11) [where we take into account Eq. (10)] reads $E^{\text{on}} = E_0(\psi) W^{\text{on}}$, where

$$W^{\text{on}} = 1 - \frac{\sin^2 \psi}{k^2} + \frac{4 \sin \psi}{\pi k} E(k) - 2 \cos \psi, \quad (12)$$

with $E_0(\psi) = 2\pi L \ell^2 \ln(1 + wR^{-1} \cos \psi) / \cos \psi$, and $E(k)$ is the complete elliptic integral of the second kind [28]; see Fig. 2(a).

Another (“axial”) solution of the pendulum equation reads $\phi^{\text{ax}} = \pm\pi/2$ [see Figs. 2(b) and 2(c)], which has an energy $E^{\text{ax}} = E_0(\psi)W^{\text{ax}}$, with $W^{\text{ax}} = \cos^2 \psi$. The equality of the energies $W^{\text{on}}(\psi) = W^{\text{ax}}(\psi)$ determines some critical angle $\psi_c \approx 0.8741 \approx 5\pi/18$ which separates the onion ($\psi < \psi_c$) and axial ($\psi > \psi_c$) phases; see Fig. 2(a).

The obtained evolution of the equilibrium states with the curvature changing (increasing of ψ) is a manifestation of the above-mentioned interplay of two geometries: the geometry of the vector field (magnetization vector) and the geometry of the magnetic shell. The energy \mathcal{E}^t consists of three competitive interactions: a “standard” exchange $\mathcal{E}_0^t = (\nabla\phi)^2$ which homogenizes the spatial distribution of the magnetization vector, and two terms that are due to a nontrivial geometrical structure of the shell, namely, an effective anisotropy interaction $\mathcal{E}_A^t = \Gamma^2$ and an effective Dzyaloshinskii-like [30] $\mathcal{E}_D^t = -2(\nabla\phi \cdot \Omega)$ interaction. For the cone surface the anisotropy term $\mathcal{E}_A^t = g^{-1} \sin^2 \psi \cos^2 \phi$ dominates for surfaces close to cylindrical ($\psi \rightarrow \pi/2$) and it makes the axial solution $\phi = \pm\pi/2$ energetically more favorable, while the Dzyaloshinskii interaction $\mathcal{E}_D^t = -2g^{-1} \cos \psi \partial_\chi \phi$ dominates for cone surfaces close to planar, $|\psi| \ll \psi_c$, and it favors the spatially inhomogeneous distribution given by the solution (11).

It should be noted that the appearance of the curvature-induced Dzyaloshinskii-like term can explain the observed polarity [31,32] and chirality [33] symmetry breaking for magnetic vortices caused by the surface roughness.

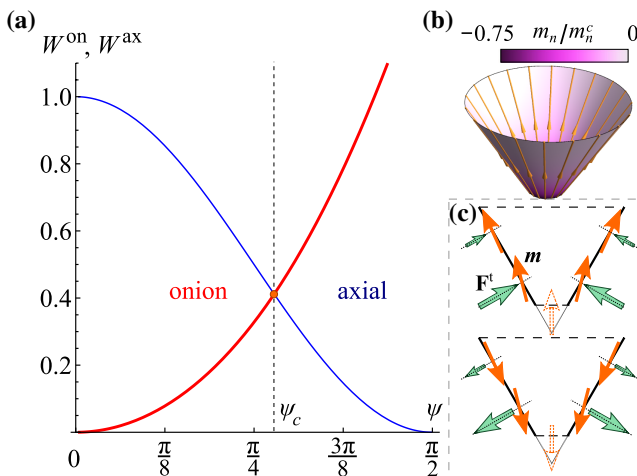


FIG. 2 (Color online) (color online). a) Energies of the onion (thick line) and axial (thin line) solutions. The magnetization distributions of the axial-state cone with $\psi = \pi/3$ are shown precisely and schematically in panels b) and c), respectively. The other notations are the same as in Fig. 1.

The curvature-induced out-of-surface deviations of the magnetization vector given by Eq. (6) with the effective field $\mathbf{F}^t = \mathbf{n} \sin \psi \sin \phi (2\partial_\chi \phi - \cos \psi) / g$ are shown in Figs. 1(c) and 2(b) for the cases of the onion and axial solutions, respectively. The corresponding distributions of the effective field \mathbf{F}^t are shown, respectively, in Figs. 1(e) and 2(c). These results demonstrate that the magnetization vector deviates from the surface mostly in the vicinity of the cone vertex. Far away from the vertex the deviation is small. The reason for such a behavior is a competition between the exchange and the easy-surface anisotropy. The effective magnetic field \mathbf{F}^t originates from the exchange energy. In the case of a cone surface it is proportional to the square of the mean curvature $\mathcal{H}^2 \sim g^{-1}$ and it is maximal near the cone vertex. As the distance from the vertex increases the mean curvature \mathcal{H} decreases, and the easy-surface anisotropy interaction prevails and makes the magnetization distribution essentially tangential. It is worth noticing that the out-of-surface deviations are absent in planar shells ($\psi \rightarrow 0$) as well as for axial states of cylindrical shells ($\psi \rightarrow \pi/2$, $\phi = \pm\pi/2$), since in these cases $\mathbf{F}^t \equiv 0$.

In magnetic shells with a strong easy-normal anisotropy the magnetization is oriented along the normal vector (inward or outward from the cone surface) up to the small deviations (8) originating from the curvature-induced effective magnetic field $\mathbf{F}^n = g^{-1} \sin \psi \cos \psi \tau(\phi)$, where $\phi = \pi/2$ for the inward and $\phi = -\pi/2$ for the outward magnetization directions; see Fig. 3. The appearance and spatial behavior of the out-of-normal magnetization deviations have the same qualitative explanation as in the case of an easy-surface anisotropy. Note that the deviation from the normal distribution vanishes for a cylindrical surface ($\psi = \pi/2$) as well as for the planar case ($\psi = 0$).

For both cases the order of magnitude of the deviations θ is determined by the quantity $m_n^c = \sigma^2 / R^2$. For a thin film of a magnetically soft material the effective easy-surface anisotropy has a magnetostatic nature ($\lambda = 1/2$). In the case of Permalloy ($\ell = 5.3$ nm) film one can estimate $m_n^c \approx 2.2 \times 10^{-2}$ and $m_n^c \approx 5.6 \times 10^{-3}$ for cones with a radius of $R = 50$ nm and $R = 100$ nm, respectively.

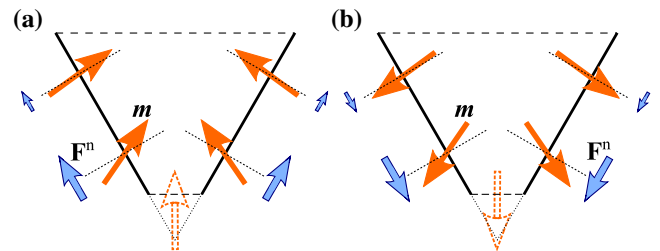


FIG. 3 (color online). Schematic representation of the magnetization \mathbf{m} and curvature-induced effective field \mathbf{F}^n distributions for the case of a strong easy-normal anisotropy, with a) inward and b) outward magnetization orientations.

The developed concept of effective curvature fields can be used to make computer simulations faster when modeling curvature effects in high-anisotropy shells: we propose to introduce the effective curvature fields \mathbf{F}^t and \mathbf{F}^n into a simulation code instead of the excessive mesh refinement in regions with small curvature radii [34].

In summary, an exchange energy functional for thin arbitrary curved magnetic shells with easy-surface and easy-normal magnetic anisotropy have been derived and general solutions for static magnetization distributions were discussed. It is shown that the effect of the curvature can be treated as the appearance of an effective magnetic field. The means of the developed general theory were demonstrated for a cone surface.

The authors thank D. Makarov for stimulating discussions and acknowledge the IFW Dresden, where part of this work was performed, for kind hospitality. This work was partially supported by DFG project MA 5144/3-1, and by the Grant of the President of Ukraine for the support of researches of young scientists (Project No GP/F49/083).

*ybg@bitp.kiev.ua

†Corresponding author.

vkravchuk@bitp.kiev.ua

‡sheka@univ.net.ua

- [1] O. G. Schmidt and K. Eberl, *Nature (London)* **410**, 168 (2001).
- [2] H.-C. Yuan, Z. Ma, M. M. Roberts, D. E. Savage, and M. G. Lagally, *J. Appl. Phys.* **100**, 013708 (2006).
- [3] D.-H. Kim, J.-H. Ahn, W. M. Choi, H.-S. Kim, T.-H. Kim, J. Song, Y. Y. Huang, Z. Liu, C. Lu, and J. A. Rogers, *Science* **320**, 507 (2008).
- [4] F. Balhorn, S. Mansfeld, A. Krohn, J. Topp, W. Hansen, D. Heitmann, and S. Mendach, *Phys. Rev. Lett.* **104**, 037205 (2010).
- [5] R. Streubel, D. J. Thurmer, D. Makarov, F. Kronast, T. Kosub, V. Kravchuk, D. D. Sheka, Y. Gaididei, R. Schaefer, and O. G. Schmidt, *Nano Lett.* **12**, 3961 (2012).
- [6] R. C. T. da Costa, *Phys. Rev. A* **23**, 1982 (1981).
- [7] M. Burgess and B. Jensen, *Phys. Rev. A* **48**, 1861 (1993); Y. B. Gaididei, S. Mingaleev, and P. L. Christiansen, *Phys. Rev. E* **62**, R53 (2000); M. V. Entin and L. I. Magarill, *Phys. Rev. B* **66**, 205308 (2002); C. Gorria, Y. B. Gaididei, M. P. Soerensen, P. L. Christiansen, and J. G. Caputo, *Phys. Rev. B* **69**, 134506 (2004); Y. B. Gaididei, P. L. Christiansen, P. G. Kevrekidis, H. Büttner, and A. R. Bishop, *New J. Phys.* **7**, 52 (2005); G. Ferrari and G. Cuoghi, *Phys. Rev. Lett.* **100**, 230403 (2008); B. Jensen and R. Dandoloff, *Phys. Rev. A* **80**, 052109 (2009); G. Cuoghi, G. Ferrari, and A. Bertoni, *Phys. Rev. B* **79**, 073410 (2009); A. P. Korte and G. H. M. van der Heijden, *J. Phys. Condens. Matter* **21**, 495301 (2009); S. Bittner, B. Dietz, M. Miski-Oglu, A. Richter, C. Ripp, E. Sadurní, and W. P. Schleich, *Phys. Rev. E* **87**, 042912 (2013).
- [8] M. J. Bowick and L. Giomi, *Adv. Phys.* **58**, 449 (2009).
- [9] A. M. Turner, V. Vitelli, and D. R. Nelson, *Rev. Mod. Phys.* **82**, 1301 (2010).
- [10] M. J. Bowick, D. R. Nelson, and A. Travesset, *Phys. Rev. B* **62**, 8738 (2000).
- [11] M. Bowick and A. Travesset, *J. Phys. A* **34**, 1535 (2001).
- [12] V. Vitelli and A. M. Turner, *Phys. Rev. Lett.* **93**, 215301 (2004).
- [13] T. Lopez-Leon, V. Koning, K. B. S. Devaiah, V. Vitelli, and A. Fernandez-Nieves, *Nat. Phys.* **7**, 391 (2011).
- [14] G. Napoli and L. Vergori, *Phys. Rev. Lett.* **108**, 207803 (2012).
- [15] G. Napoli and L. Vergori, *Phys. Rev. E* **85**, 061701 (2012).
- [16] P. Landeros and Á. S. Núñez, *J. Appl. Phys.* **108**, 033917 (2010).
- [17] A. González, P. Landeros, and Á. S. Núñez, *J. Magn. Magn. Mater.* **322**, 530 (2010).
- [18] V. P. Kravchuk, D. D. Sheka, R. Streubel, D. Makarov, O. G. Schmidt, and Y. Gaididei, *Phys. Rev. B* **85**, 144433 (2012).
- [19] E. J. Smith, D. Makarov, S. Sanchez, V. M. Fomin, and O. G. Schmidt, *Phys. Rev. Lett.* **107**, 097204 (2011).
- [20] M. Albrecht, G. Hu, I. L. Guhr, T. C. Ulbrich, J. Boneberg, P. Leiderer, and G. Schatz, *Nat. Mater.* **4**, 203 (2005).
- [21] T. C. Ulbrich, D. Makarov, G. Hu, I. L. Guhr, D. Suess, T. Schrefl, and M. Albrecht, *Phys. Rev. Lett.* **96**, 077202 (2006).
- [22] G. Gioia and R. D. James, *Proc. R. Soc. A* **453**, 213 (1997).
- [23] R. Kohn and V. Slastikov, *Proc. R. Soc. A* **461**, 143 (2005).
- [24] R. V. Kohn and V. V. Slastikov, *Arch. Ration. Mech. Anal.* **178**, 227 (2005).
- [25] V. Slastikov, *Math. Models Methods Appl. Sci.* **15**, 1469 (2005).
- [26] Note that the spin connection Ω vanishes in the Cartesian frame of reference, but in the general case of an arbitrary curvilinear basis $\Omega \neq 0$, even in the planar case.
- [27] M. Kläui, C. A. F. Vaz, L. Lopez-Diaz, and J. A. C. Bland, *J. Phys. Condens. Matter* **15**, R985 (2003).
- [28] *NIST Handbook of Mathematical Functions*, edited by F. W. J. Olver, D. W. Lozier, R. F. Boisvert, and C. W. Clark (Cambridge University Press, Cambridge, England, 2010).
- [29] This result is valid for an infinitely thin shell. In the case of finite thickness the influence of edge magnetostatic charges deforms the uniform magnetization, resulting in the onion state [27] typical for this geometry.
- [30] I. E. Dzialoshinskii, *Sov. Phys. JETP* **5**, 1259 (1957); I. Dzyaloshinsky, *J. Phys. Chem. Solids* **4**, 241 (1958).
- [31] K. W. Chou, A. Puzic, H. Stoll, D. Dolgos, G. Schutz, B. V. Waeyenberge, A. Vansteenkiste, T. Tyliczszak, G. Woltersdorf, and C. H. Back, *Appl. Phys. Lett.* **90**, 202505 (2007).
- [32] M. Curcic, B. V. Waeyenberge, A. Vansteenkiste, M. Weigand, V. Sackmann, H. Stoll, M. Fähnle, T. Tyliczszak, G. Woltersdorf, C. H. Back, and G. Schütz, *Phys. Rev. Lett.* **101**, 197204 (2008).
- [33] A. Vansteenkiste, M. Weigand, M. Curcic, H. Stoll, G. Schtz, and B. V. Waeyenberge, *New J. Phys.* **11**, 063006 (2009).
- [34] To avoid possible nonphysical effects the simulated curvilinear surface must be smooth enough, which requires a rather detailed mesh; hence, the modeling becomes very expensive from a computational point of view.